Using Advanced Imaging Methods to Study Neurolathyrism

Atira S. Bick PhD, Zeev Meiner MD, Marc Gotkine MBBS and Netta Levin MD PhD

fMRI Unit, Department of Neurology, Hadassah Hebrew-University Medical Center, Jerusalem, Israel

ABSTRACT: **Background:** Neurolathyrism is a toxic nutritional disorder caused by consumption of the grass pea, *Lathyrus sativus*. The disease, which manifests as an acute or insidiously evolving spastic paraparesis, continues to occur throughout Africa and Asia. Research on this disease is limited, and to our knowledge no imaging studies of patients with neurolathyrism have been published.

Objectives: To better localize the site of damage in neurolathyrism using advanced imaging methods.

Methods: Three male patients, immigrants from Ethiopia, were included in the study. All had a history of arrested spastic paraparesis that had evolved before their emigration from Ethiopia, and a past history of exposure to grass pea without any other cause. Functional magnetic resonance imaging (fMRI) included simple motor tasks to evaluate cortical motor areas. Anatomic scans included diffusion tensor imaging (DTI) to evaluate the corticospinal tracts.

Results: In all patients clear activation was found in motor regions, and the patients' activity pattern was qualitatively similar to that in control subjects. In one patient in whom clinical symptoms were asymmetric, an asymmetric activity pattern in M1 was identified. DTI analysis identified intact corticospinal tracts connecting the pons and the primary motor regions, similar to control subjects.

Conclusions: Advanced neuroimaging clearly identified well-functioning motor regions and tracts in neurolathyrism patients, suggesting a spinal etiology.

IMAJ 2016; 18: 341–345

KEY WORDS: neurolathyrism, grass pea, functional magnetic resonance imaging (fMRI), diffusion tensor imaging (DTI)

Neurolathyrism is a neurodegenerative disease caused by heavy consumption of the grass pea, *Lathyrus sativus* [1]. The pea contains large amounts of the neurotoxin, β-N-oxalyl-L-α,β-diaminopropionic acid (L-β-ODAP), an AMPA receptor agonist of ionotropic glutamate receptors. Sustained stimulation of the glutamate receptors causes excitotoxicity. This, together with nitric oxide over-production, causes irreparable damage to mitochondria and cellular macromolecules leading to motor neuron degeneration [2]. Neurolathyrism is one of the oldest known neurotoxic diseases, and was already described by Hippocrates. The grass pea is drought-resistant and is thus consumed in large amounts during times of famine. Epidemics have continued to occur in recent decades throughout Africa and Asia, including Ethiopia where it is especially common in the northwest (prevalence rates ranged from 1/10,000 to 7.5/1000 in the 1990s) [3].

Corticospinal involvement leading to spastic paraparesis is characteristic. Only in the most severe cases are the upper limbs affected. Risk factors include male gender, young age, and concurrent malnutrition [4]. The degree of a patient's disability was categorized into four stages: from no need for a walking stick, through the need for one or two walking sticks, to the final stage, crawling [5].

Histopathological reports in neurolathyrism are rare. Involvement of the thoracolumbar and lumbar region of the spinal cord has been reported [6]. Other histopathological changes in lathyrism include degeneration of Betz cells in the cerebral cortex, loss of myelin and axons in the pyramidal tract, swelling and degeneration of anterior horn cells, and swelling of Goll's nuclei (gracile nucleus) [7,8]. Since the disease occurs in areas with limited medical services, many aspects of the disease have yet to be investigated. No functional imaging studies of patients with neurolathyrism have been performed.

The aim of the current study was to better localize the site of damage in neurolathyrism using advanced imaging methods: functional magnetic resonance imaging (fMRI) and diffusion tensor imaging (DTI). Identifying the site of the lesion is essential to understand the mechanism involved and to determine possible remedies.

PATIENTS AND METHODS

Three patients diagnosed with neurolathyrism were studied. The patients, males aged 26–40 years, were all immigrants from Ethiopia. Case definition for neurolathyrism included symmetric spastic leg weakness, sub-acute or insidious onset, no sensory deficit, and history of grass pea consumption prior to and at the onset of paralysis. Two right-handed healthy male subjects (age 28 and 36) without any neurological background participated as control subjects. The imaging procedure was identical

for patients and controls. Procedures followed the tenets of the Declaration of Helsinki and written informed consent was obtained from all participants.

DATA ACQUISITION

The blood oxygenation level-dependent (BOLD) fMRI measurements were performed in a whole-body 3T Siemens scanner. BOLD contrast was obtained with a gradient-echo echo-planar imaging sequence and a standard head coil. Functional data were obtained using TR 2 s, TE 30 ms, flip angle 90°, imaging matrix 80 x 80, field of vision (FOV) 22 x 22 cm (inplane resolution 2.75 x 2.75 mm) and 30 slices, 3 mm each with 0.5 mm gap between slices. Slices were placed oblique to cover most of the brain. DTI data were acquired using a diffusion-weighted imaging sequence (single shot, spin echo, TE 94 ms, TR 7127–8224 ms). To cover the whole brain, 52–60 axial 2 mm thick slices (no skip) were acquired, matrix size 96 x 96; FOV 288 mm (inplane resolution 2*2) for two b values, b = 0 and b = 1000 s/mm^2. The high b value was obtained by applying gradients along 64 different diffusion directions, including 2 averages. Anatomical MRI sequences included a high resolution T1-weighted MPRAGE sequence: minimum TE, flip angle 9°, TR 2300 ms, voxel size 1*1*1.1 mm.

FMRI EXPERIMENTAL PARADIGM

Subjects were required to open and close their hand and to perform flexion/extension of the ankle. Motor tasks were executed separately for each body side. Conditions were interleaved, and each was repeated four times in a counterbalanced manner in an fMRI block-designed experiment (12 s blocks, 9 s rest; a dummy block was inserted at the beginning of the experiment and removed during the analysis). The hands and feet were activated in different runs for one patient, but in the same run for the others. Counterbalancing assured that subjects could not predict the next movement and could not alter cortical activity in a movement-specific manner. A short auditory instruction was given at the beginning and at the end of each block, stating which movement to execute (e.g., "right hand" or "left foot") and when to rest ("stop"). For all participants except one (case 1) the frequency of movement was controlled: auditory instructions informed the pace of movements within a block (0.5 Hz). Six movements of the same type were performed within each block.

A simple motor task was chosen, so that both patients and control would be able to adequately perform the task. This task is used in routine clinical presurgery evaluation and achieves robust activation in the primary motor cortex (M1), the supplementary motor area (SMA), and commonly also in the cerebellum. For two patients the motor task was followed by an identical session in which they were asked to imagine the motion rather than actually perform it.

Auditory instructions were presented using the NNL (NordicNeuroLab) auditory system including noise attenuation of +30 dB. The language of instructions was tailored to each participant, and therefore an Amharic version was prepared and used by two of the patients. Stimulus presentation was implemented with Presentation software (http://www.neurobs.com/presentation).

DATA ANALYSIS

fMRI data analysis was performed using the BrainVoyager QX software package (Brain Innovation, Maastricht, The Netherlands, 2000). Prior to the statistical analysis, the raw data were examined for motion and signal artifacts. Head motion correction and high-pass temporal filtering in the frequency domain (three cycles/total scan time) were applied to remove drifts and improve the signal-to-noise ratio. Functional images were registered and incorporated into the three-dimensional data sets through tri-linear interpolation. Automatic registration was inspected and adjusted manually.

Changes in BOLD contrast associated with the performance were assessed on a pixel-by-pixel basis, using the general linear model (GLM) [9]; the hemodynamic response function was modeled using standard parameters [11]. Motion correction parameters were included in the GLM to correct for the patient's movements.

DTI image processing and analysis were performed using the open-source mrVista package http://vistalab.stanford.edu/software. Preprocessing included removing Eddy current distortions and subject motion. Each diffusion-weighted image was then registered to the mean of the (motion-corrected) non diffusion-weighted images using a two-stage coarse-to-fine approach that maximized the normalized mutual information. The mean of the non-diffusion weighted images was also automatically aligned to the T1 image using a rigid body mutual information algorithm.

Probabilistic fiber tractography was used to delineate the motor pathways in each patient. Fiber tracking was performed using the Contrack algorithm [11], a probabilistic algorithm designed to find the most likely pathway between two regions of interest (ROI). Fibers were identified in right and left hemispheres independently. The first ROI was positioned on T1 maps and three color tensor maps of each subject, centered on motor pons. The volume of these regions were standardized to 485 mm^3 (5 mm sphere). The second ROI was defined in the primary motor cortex using fMRI. ConTrack was set to generate a set of 50,000 candidate pathways between the ROIs. The candidate pathways were scored, and the top 20% (10,000) highest scored pathways were selected as the most likely pathways for connecting the pons and the primary motor cortex. A few clearly misidentified fibers were eliminated by visual inspection.

DIFFUSIVITY MEASUREMENTS

The tensors were fitted using a least-squares algorithm. The eigenvalue decomposition of the diffusion tensor was computed. Measures of the mean diffusivity (MD), the fractional anisotropy (FA), and diffusion parallel axial diffusivity (AD)

and perpendicular radial diffusivity (RD) to the principal fiber direction were derived.

DIFFUSIVITY MEASUREMENTS ALONG THE TRACT AND CORE FIBER ANALYSIS

In order to avoid partial voluming with non-white matter (i.e., ventricles or grey matter), diffusion measurements were taken near the dense core of the fibers. Diffusion at the core was estimated by combining data from different voxels in a weighted fashion, assigning greater weight to voxels that are close to the core of the estimated tract [12]. Diffusion measures along the tract were re-sampled at 50 positions, calculating FA and the MD, AD and RD at each of these nodes. In this way, measures throughout the length of the fiber could be combined across different subjects.

RESULTS

Patients' characteristics are summarized in Table 1.

Table 1. Patients' characteristics **[A]** and clinical evaluation **[B]**

A

Patient	Age	Gender	Age of onset (year)	Type of onset	Motor disability
Case 1	26	M	5	Days–weeks	Unstable walking
Case 2	40	M	31	3 months	Wheelchair
Case 3	33	M	28	unclear	Walking with 2 crutches

B

Patient	Legs					Hands
	Spasticity (Modified Ashworth Scale)	Proximal strength	Distal strength	Tendon reflexes	Pyramidal signs	
1	3/4	3/5	3/5	+++	+	-
2	4/4	1–2/5	1–2/5	+++	+	-
3	3/4	2–3/5	2–3/5	+++	+	+

PATIENT 1

A 26 year old male was evaluated for a 21 year history of bilateral lower limb spasticity. He developed acute-onset spastic bilateral lower limb weakness that progressed rapidly over days to weeks and then plateaued over the following years. No sphincter involvement was described. Examination revealed intact cranial nerves and upper limbs. Lower limb spasticity was of moderate severity with brisk deep tendon reflexes, bilateral positive Babinski sign and sustained bilateral clonus. Gait was spastic. There was no sensory deficit. Whole-spine MRI was normal. A muscle relaxant (baclofen 100 mg daily) was prescribed with only mild amelioration of the spasticity. At the time of the study he was in stage 1 of the patient's disability scale [5].

PATIENT 2

A 40 year old male was evaluated for a 9 year history of gait disturbance. He developed spastic bilateral lower limb weakness that progressed rapidly over 3 months, after which he was wheelchair-bound. There were no sensory, sphincter or sexual dysfunction symptoms. Examination revealed intact cranial nerves. Tone was increased in the legs only, associated with sustained clonus, right Babinski and right Hoffman signs. Marked flexor contractures were evident in both knees and ankles. Brain and cervical MRI scans as well as cerebrospinal content (evaluated for cells, biochemistry and oligoclonal bands) were normal. At the time of the study he was in stage 4 of the patient's disability scale [5].

PATIENT 3

A 33 year old male was evaluated for a 5 year history of lower limb spastic paresis with milder upper limb pyramidal signs. Detrusor hyper-reactivity was also described. Examination revealed spastic weakness in all four limbs, legs more than hands, accompanied by brisk deep tendon reflexes, bilateral positive Babinski sign and sustained bilateral clonus. Gait was very spastic and required two crutches. At the time of the study he was in stage 3 of the patient's disability scale [5].

All three patients had lived in an area of Ethiopia with high grass pea consumption, where the disease was known to be endemic.

CORTICAL MOTOR MAPS

Movement of the hands activated expected regions in the primary motor cortex, SMA and cerebellum in the control subjects as well as the patients [Figure 1]. In one patient (# 3) an artifact was highly correlated with activation related to movement of the left hand. Since it was impossible to differentiate between the actual signal and the artifact, these data were removed

Figure 1. Cortical activation related to hand movements. Activation related to motion of the hand in primary motor cortex (marked with yellow arrow) and SMA (marked with red arrow) is overlaid on axial T1 slice. Activation for patients (right) did not differ from controls (left)

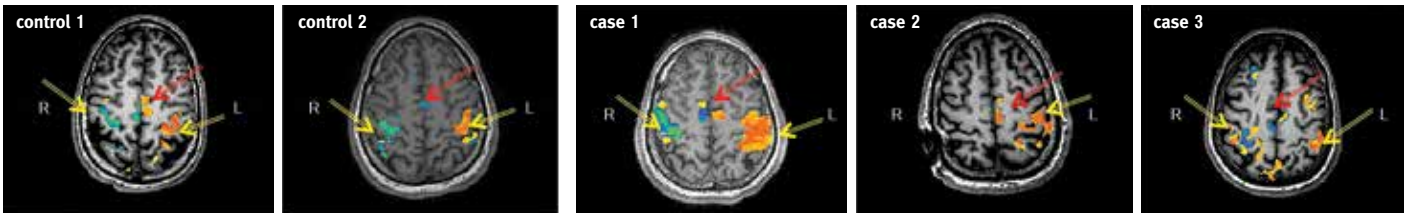

Figure 2. Cortical activation related to foot movements. Activation related to motion of the foot in primary motor cortex (marked with yellow arrow) is overlaid on axial T1 slice. Activation for patients (right) did not differ from controls (left)

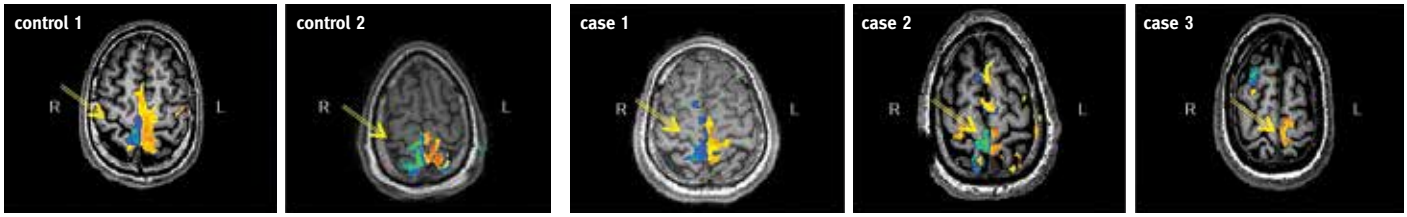

from the analysis. Cerebral activation was in the contralateral hemisphere to the activated limb. The extent of activation differed between subjects, but no systematic difference could be observed between patients and controls.

Movement of the feet activated expected regions in the primary motor cortex in control subjects and two of the patients [Figure 2]. In one patient (# 2) no response to motion of the right limb was identified. Since motion was not recorded it is impossible to determine whether this result is related to difficulty in performing the task or to disrupted neural representation. The extent of activation differed between subjects, but no systematic difference could be observed between patients and controls.

The motor imagery task, which activated regions in the motor cortex in control subjects, did not elicit any significant activation in any of the patients because of cultural differences and inadequate translation. Therefore, this task was discarded.

CORTICOSPINAL FIBERS

DTI was performed in two patients. DTI tractography was able to clearly reconstruct the corticospinal motor fibers connecting the pons with the primary motor cortex in both patients. Fiber did not differ from those of the controls [Figure 3 A & B]. Analysis of microstructure diffusion properties found similar values for both patients and controls [Figure 3C]. FA analysis showed that diffusion levels were similar for both hands (left hand: 0.55 in patient 2, 0.5 in patient 1, 0.48 in control 1, 0.56 in control 2; right hand: 0.65 in patient 2, 0.58 in patient 1, 0.54 in control 1, 0.67 in control 2) and feet (left foot: 0.49 in patient 1, 0.45 in control 1, 0.52 in control 2; right foot: 0.62 in patient 2, 0.56 in patient 1, 0.52 in control 1, 0.6 in control 2). A similar pattern of results was found for the other diffusion measures: AD, MD and RD.

DISCUSSION

In two patients clear symmetric activation was found in motor regions, including primary motor cortex (M1), cerebellum and supplementary motor area (SMA). The activity pattern was qualitatively similar to control subjects. In one patient (# 2), in whom clinical symptoms were asymmetric with positive Babinski and positive Hoffman's sign only on the right, an asymmetric activity pattern in M1 was identified. Response to movements of the hands in the left hemisphere (contralateral to the weaker side) was limited relative to the right hemisphere. His

Figure 3. Corticospinal fibers. Fibers reaching a region involved in motion of the foot (in blue) and fibers reaching a region involved in motion of the hand (in green) were similar for controls **[A]** and patients **[B]**. Fibers are presented on coronal T1 slice. Microstructure analysis of corticospinal tracts did not yield any systematic differences between average FA of patients and controls for hands or feet **[C]**

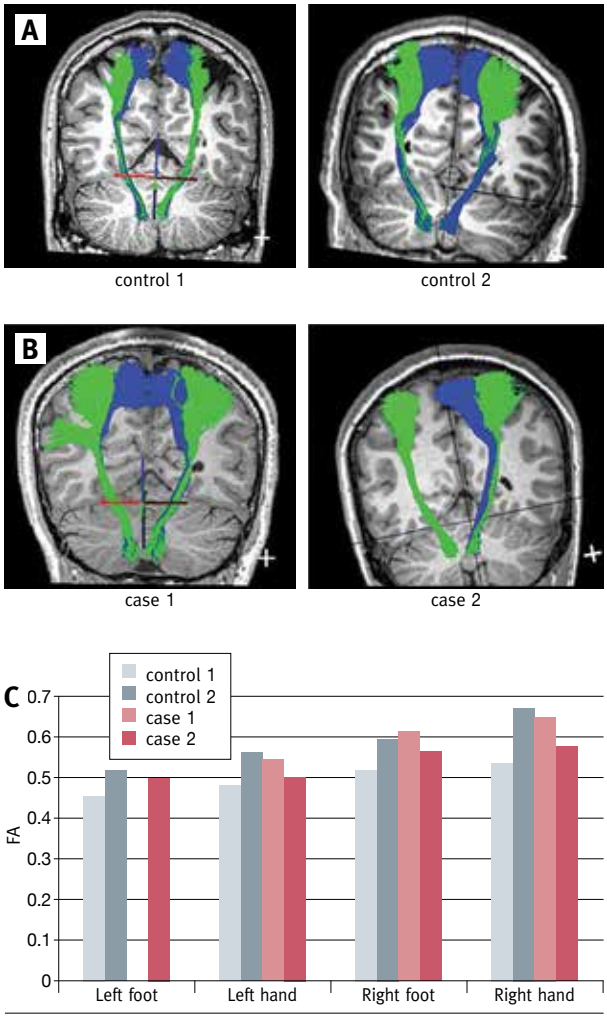

asymmetric pattern of activity in primary regions was accompanied by a symmetric pattern in secondary motor regions – the SMA and cerebellum.

DTI analysis identified the corticospinal tracts connecting the pons and the primary motor regions. Macro- as well as micro-structurally, the tracts seemed intact and similar to those of the control subjects. Thus, it seems that the advanced neuroimaging methods used here did not allow us to identify a pattern characteristic of neurolathyrism.

Other motor neuron diseases studied with MRI, such as amyotrophic lateral sclerosis (ALS) and hereditary spastic paraparesis (HSP), showed differences between patients and controls. An increase in fMRI activation in ipsi- and contralateral primary motor regions as well as in the SMA, basal ganglia and cerebellum was identified in ALS [13]. In HSP inconsistent results were reported [14] and effects were shown to be dependent on task and performance [15]. Thus, since patients usually comprise a heterogeneous group, differing in their individual effort during the task, it is hard to untangle motor capabilities and cortical plasticity. Using DTI, decreased FA in regions in the corticospinal tracts and corpus callosum were reported in ALS and HSP patients [16]. Yet, these differences were not sufficient to enable the use of DTI for diagnosis in ALS (for meta-analysis, see [17]).

Our results suggest that the neuropathology in neurolathyrism differs from that in ALS and HSP in both white and grey matter. The limited pathology studies conducted in neurolathyrism patients suggested several locations along the entire motor system as the primary site of damage [7,8]. Our results showing no consistent differences within either the motor cortex or the upper portion of the corticospinal tracts may indicate dominant involvement of spinal pathology relative to central pathology. The selective susceptibility of spinal motor neurons to AMPA receptor activation [18] and the lack of bulbar/pseudo-bulbar involvement in the disease may further support this assumption.

Several methodological considerations should be noted. As mentioned above, an inherent challenge of motor research and especially research of motor diseases is separating the neural representation of motor effort, motor abilities and plasticity effects due to damage. A common solution is the use of imagery. Motor imagery was indeed included in the original design of the study; however, no reliable results could be identified in any of the patients. This may be due to cultural barriers.

Neurolathyrism is rarely encountered in centers where advanced imaging techniques are available. Therefore, the number of patients in this study was limited. Moreover, there are no clear diagnostic criteria for the disease, and diagnosis is based solely on clinical features after excluding other etiologies. Although we believe neurolathyrism was the most likely diagnosis in all these cases, we cannot rule out the possibility that an alternative etiology was responsible for the motor disorder.

To our knowledge, this is first time neurolathyrism has been investigated using advanced imaging techniques. The fact that no clear abnormality in brain function was observed in these patients may indicate that the disease primarily results from axonal dysfunction at the spinal level, with relative preservation of the cortical cell bodies. Further research, particularly pathology studies, would help establish this hypothesis.

Correspondence

Dr. N. Levin

fMRI Lab, Dept. of Neurology, Hadassah-Hebrew University Medical Center, P.O. Box 12000, Jerusalem 91120, Israel

Phone: (972-2) 677-8476

Fax: (972-2) 642-1203

email: netta@hadassah.org.il

References

1. Woldeamanuel YW, Hassan A, Zenebe G. Neurolathyrism: two Ethiopian case reports and review of the literature. *J Neurol* 2012; 259 (7): 1263-8.
2. Khandare AL, Ankulu M, Aparna N. Role of glutamate and nitric oxide in onset of motor neuron degeneration in neurolathyrism. *Neurotoxicology* 2013; 34: 269-74.
3. Haimanot RT, Kidane Y, Wuhib E, et al. The epidemiology of lathyrism in north and central Ethiopia. *Ethiop Med J* 1993; 31 (1): 15-24.
4. Misra UK, Sharma VP, Singh VP. Clinical aspects of neurolathyrism in Unnao, India. *Paraplegia* 1993 31 (4): 249-54.
5. Getahun H, Lambein F, Vanhoorne M, Van der Stuyft P. Pattern and associated factors of the neurolathyrism epidemic in Ethiopia. *Trop Med Int Health* 2002; 7 (2): 118-24.
6. Sachdev S, Sachdev JC, Puri D. Morphological study in a case of lathyrism. *J Indian Med Assoc* 1969; 52 (7): 320-2.
7. Striefler M, Cohn DF, Hirano A, Schujman E. The central nervous system in a case of neurolathyrism. *Neurology* 1977; 27 (12): 1176-8.
8. Shrivastava KK, Sarasa Bharati R, Arora MM. Rare postmortem findings in a case of human lathyrism. *Indian J Pathol Microbiol* 1982; 25 (3): 225-8.
9. Friston KJ, Frith CD, Turner R, Frackowiak RS. Characterizing evoked hemodynamics with fMRI. *Neuroimage* 1995; 2 (2): 157-65.
10. Boynton GM, Engel SA, Glover GH, Heeger DJ. Linear systems analysis of functional magnetic resonance imaging in human V1. *J Neurosci* 1996; 16 (13): 4207-21.
11. Sherbondy AJ, Dougherty RF, Ben-Shachar M, Napel S, Wandell BA. ConTrack: finding the most likely pathways between brain regions using diffusion tractography. *J Vis* 2008; 8 (9): 15.1-16.
12. Yeatman JD, Dougherty RF, Myall NJ, Wandell BA, Feldman HM. Tract profiles of white matter properties: automating fiber-tract quantification. *PLoS One* 2012; 7 (11): e49790.
13. Kollewe K, Korner S, Dengler R, Petri S, Mohammadi B. Magnetic resonance imaging in amyotrophic lateral sclerosis. *Neurol Res Int* 2012; 2012: 608501.
14. Tomberg T, Braschinsky M, Rannikmae K, et al. Functional MRI of the cortical sensorimotor system in patients with hereditary spastic paraplegia. *Spinal Cord* 2012; 50 (12): 885-90.
15. Koritnik B, Azam S, Knific J, Zidar J. Functional changes of the cortical motor system in hereditary spastic paraparesis. *Acta Neurol Scand* 2009; 120 (3): 182-90.
16. Muller HP, Unrath A, Huppertz HJ, Ludolph AC, Kassubek J. Neuroanatomical patterns of cerebral white matter involvement in different motor neuron diseases as studied by diffusion tensor imaging analysis. *Amyotroph Lateral Scler* 2012; 13 (3): 254-64.
17. Foerster BR, Dwamena BA, Petrou M, et al. Diagnostic accuracy of diffusion tensor imaging in amyotrophic lateral sclerosis: a systematic review and individual patient data meta-analysis. *Acad Radiol* 2013; 20 (9): 1099-106.
18. Vandenberghe W, Robberecht W, Brorson JR. AMPA receptor calcium permeability, GluR2 expression, and selective motoneuron vulnerability. *J Neurosci* 2000; 20 (1): 123-32.